Combined LDA and LDA-1/2 method to obtain defect formation energies in large silicon supercells

Filipe Matusalem,[1,*] Mauro Ribeiro, Jr.,[1] Marcelo Marques,[1] Ronaldo R. Pelá,[1] Luiz G. Ferreira,[2,1] and Lara K. Teles[1]

[1]*Grupo de Materiais Semicondutores e Nanotecnologia, Instituto Tecnológico de Aeronáutica, 12228-900 São José dos Campos/SP, Brazil*

[2]*Departamento de Física dos Materiais e Mecânica, Instituto de Física, Universidade de São Paulo (USP), 05315-970 São Paulo/SP, Brazil*

(Received 23 September 2013; revised manuscript received 31 October 2013; published 10 December 2013)

A source of uncertainty in the state of the art calculations of defect levels is the inaccurate prediction of band-gap energies. Several approaches were developed to surpass this problem. However, another source of uncertainty remains: the small number of clustered atoms imposed by the computational restrictions. In this work, the LDA-1/2 method is explored in an attempt to overcome both problems with a small computational cost. We considered the self-interstitial defects in silicon as a benchmark for calculating defect states and charge-transition levels of point defects in semiconductors. We found neutral formation energies, including reaction barriers, of 4.65, 4.49, and 4.87 eV, for hexagonal, split $\langle 110 \rangle$ and C_{3v} configurations, respectively, in good agreement with most experimental results.

DOI: 10.1103/PhysRevB.88.224102 PACS number(s): 31.15.A−, 71.55.Ak, 71.15.Qe, 72.20.My

I. INTRODUCTION

The physical properties of most semiconductor materials, ranging from conductivity to optical activity, are critically affected by point defects. The concentration of defects and the position of the transition levels with respect to the band edges of the host material determine the effects on the electrical and optical properties of the host. A different combination of experimental techniques is frequently necessary for identification and characterization of these properties.[1] On the other hand, from the theoretical point of view, first-principles calculations can predict quantitatively some key properties of defects. However, the usual toolkit in these approaches, the density functional theory (DFT), in its standard implementations—the local density approximation (LDA)[2] [or its slight modification, the generalized gradient approximation (GGA)],[3] combined with supercell band structure calculations, has some limitations. While LDA and GGA have predicted many ground-state properties with good accuracy, electronic properties such as band gaps are significantly smaller than experiment. These discrepancies are caused by the lack of the discontinuity of the exchange-correlation potential.[4,5] Thus these approximations lead to inaccurate predictions of band gaps and defect levels and, consequently, to uncertainties in the computed defect formation energies and charge transition levels.[6–9]

Several methods for overcoming these limitations have been proposed. One of them is the GW approximation, in which one considers the energies of quasiparticles and calculates the electron self-energy in terms of perturbation theory.[10] This procedure has been quite successful achieving good accuracy and is considered now as the "state of art" in electronic structure calculations. However, it depends on how the starting calculation was performed (LDA or any type of hybrid functional, for example) and the type of GW employed, whether self-consistent (SC) or non-SC, e.g., full SC (GW), non-SC (G_0W_0), or partially SC (GW_0).[11] Moreover, it is extremely expensive computationally, and this is a major obstacle to employ such an approach to simulate defects because, as demonstrated by Puska *et al.*,[12] one needs at least a supercell of the order of 128–216 atomic sites.

Another method that has been successful in predicting the properties of defects and impurities in various materials,[13–16] is the screened hybrid functional of Heyd, Scuseria, and Ernzerhof (HSE).[17,18] In this method, a portion of the nonlocal Hartree-Fock exchange is range limited and mixed with local (LDA) or semilocal (GGA) exchange potentials. However, since the Hartree-Fock potential involves four-center integrals its implementation in plane-wave codes results in a high computational cost, and currently hybrid functional calculations take at least an order of magnitude more processing time than standard LDA calculations for systems with the same number of electrons.[19]

Recently, Ferreira *et al.*[20,21] have developed a simple, parameter-free successful procedure to calculate the excitation energy spectrum. The procedure is inspired by the old Slater transition state technique for atoms, shown to be equivalent to the inclusion of the self-energy of the quasiparticle. The method consists of calculating the self-energy as the quantum mechanical average of a "self-energy potential", which is added to the local part of the pseudopotential or to the $-2Z/r$ part of the all-electron potential. When transferred to the infinite crystal, the self-energy potential is trimmed not to extend to neighboring atoms. The trimming is made by means of a cutting function with a parameter "CUT", which is determined variationally by making the band-gap extreme.[20] As the best GW calculations, the Ferreira *et al.* method, named LDA-1/2, produces very good band gaps and electron effective masses for several semiconductor compounds and also for some complex systems, which also require a large computational cost, as alloys, interfaces for obtaining band offsets, electronic structures of magnetic semiconductors, surfaces and defects.[20–36] The technique can be used with both LDA and GGA. The great advantage in applying LDA-1/2 for defects is the low computational cost, which is comparable to standard DFT. Therefore it is feasible to apply LDA-1/2 to a very large supercell (in principle, containing as many atoms as for a standard LDA calculation) harnessing its correctness for excited states calculation.

In this work we analyze the accuracy of applying LDA-1/2 in defect calculations, choosing the self-interstitial silicon defect as a benchmark. The results were compared with GW

 ©2013 American Physical Society

results and experimental data. The paper is organized as follows. In Sec. II, we detail the methods. In Sec. III, we show the results and discussions, and finally, in Sec. IV, we summarize the article with some brief conclusions.

II. METHODS

The concentration of defects and the position of the transition levels derive, in first-principles calculations, directly from defect formation energies.[37] Defects in semiconductors can occur in different charge states and geometries. For each geometric configuration of a given defect, one particular charge state has the lowest formation energy. For silicon self-interstitial defect, for instance, the formation energy of a defect at the charge state q and configuration $R_D^{q'}$, i.e., in the D geometry obtained for a charge state q', is

$$E^f(q) = E\left(q, R_D^{q'}\right) - N\mu_{\mathrm{Si}} + q(E_v + \varepsilon_F + \Delta V), \quad (1)$$

where $E(q, R_D^{q'})$ is the total energy derived from a supercell calculation with one defect with charge q in a $R_D^{q'}$ configuration, for a supercell with N silicon atoms (including the defect atom). μ_{Si} is the silicon chemical potential calculated from a defect free supercell with $(N-1)$ atoms. The terms in brackets are refereed as the electron chemical potential, where ε_F is the difference between the Fermi level and the valence-band maximum (VBM) in the defect-containing calculation, and E_v is the VBM energy of the perfect crystal calculation. The formation energy of charged impurities takes into account that electrons are exchanged with the Fermi level, which one is referenced with respect to the E_v in the bulk. The problem in calculating E_v is that, in a supercell approach, the defect or impurity strongly affects the band structure, because the long-range nature of the Coulomb potential and the periodic boundary conditions inherent in the supercell approach. The creation of the defect gives rise to a constant shift in the potential, and this shift cannot be evaluated from supercell calculations alone since no absolute reference exists for the electrostatic potential in periodic structures.[37] The average potential in an infinite crystal which has no surface is a meaningless quantity[38] and, for charged systems, the total energy is ill-defined due to the divergence of the electrostatic potential.[39] To solve this problem a correction must be add, the ΔV term, necessary to align the reference potential in the defect-containing supercell with that in the defect-free one. The ΔV was calculated by plotting the difference between the total (including exchange-correlation) local potential of the defect-containing and the defect-free supercells along their cube diagonal lines and inspecting their value at position far away from the defect atom,[40] in each case, as can be seen in Fig. 1.

The quasiparticle energies are obtained with good accuracy with the LDA-1/2 method. Therefore we used the LDA-1/2 method combined with Rinke *et al.*'s method[9] for obtaining the formation energies directly from quasiparticle energies. The method consists in rewriting the formation energy equation for a given defect in terms of two contributions: vertical transition or electron addition energies (A), calculated by considering quasiparticle corrections, and the relaxation energy (E_{rel}) between two different geometric configurations, considering

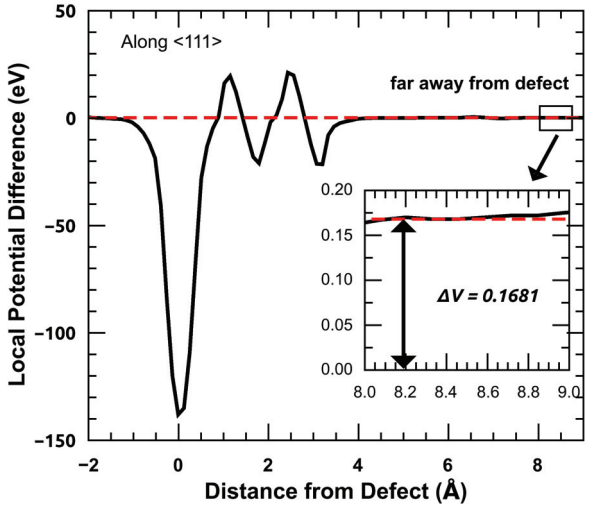

FIG. 1. (Color online) Difference between the total local potential of the defect-containing and the defect-free supercell along the diagonal line of a cubic 216-atom supercell, for a tetrahedral silicon self-interstitial defect with charge 2+. Far away from the defect atom, the local potential difference becomes constant and its value 0.1681 eV gives the correspondent ΔV correction.

the standard DFT-LDA.[9,41] The method is based on taking a determined defect charge state in such a way that the defect level in the band gap is empty. For this particular case, the formation energy calculated by standard DFT method is not so strongly affected by the band-gap problem. The other charge states configurations will be then obtained from this one by successive additions of one electron, and the formation energy obtained by successive sums of electron addition and relaxation energies, as shown schematically in Fig. 2.

Considering our benchmark case, the self-interstitial silicon defect (Si_i), one needs to consider different configurations of

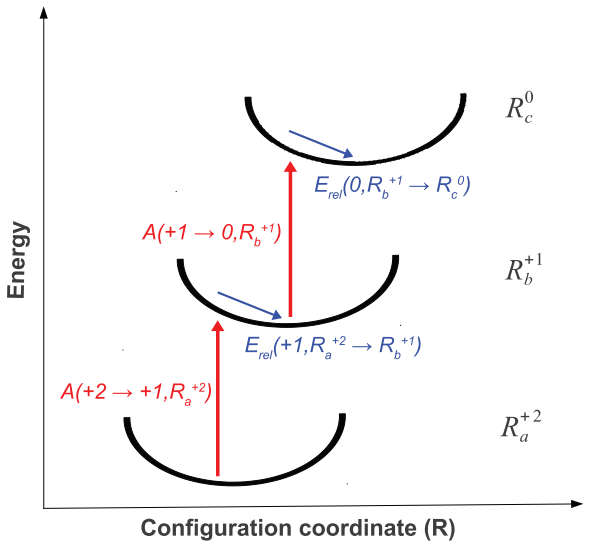

FIG. 2. (Color online) Scheme of sequential electron addition from the 2+ to neutral charge states. E_{rel}(q) is the relaxation energy for two different geometric configurations with same charge q, and $A(q \rightarrow q-1)$ is the electron addition energy from charge state q to $q-1$ in the same geometric configuration.

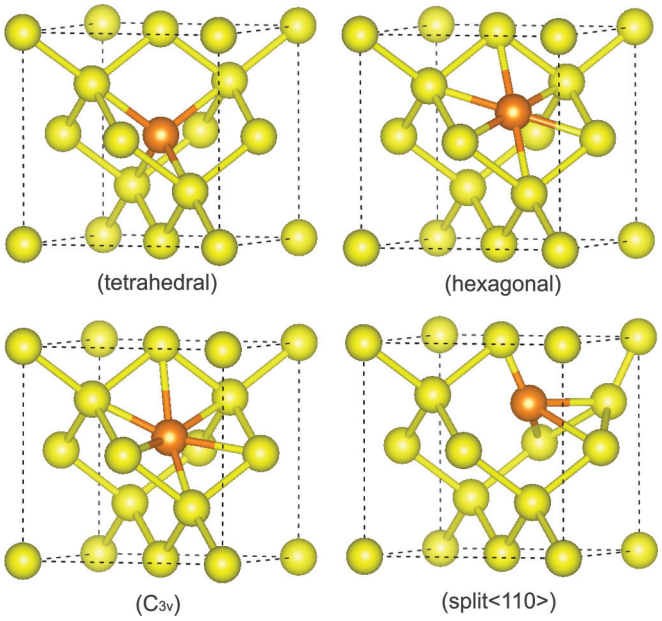

FIG. 3. (Color online) Ball-and-stick models of the different geometric configurations of silicon self-interstitial defects (orange balls) used in this work.

charge and geometry. A consensus among many theoretical calculations is that the geometries split ⟨110⟩ (split), hexagonal (hex), C_{3v} and tetrahedral (tet) defects are more stable[42] (see Fig. 3). The C_{3v} geometry is reached moving the tetrahedral defect in the ⟨111⟩ direction by about $0.12a$ (where a is the lattice parameter), and was stable only for neutral and 1− charge states. The hexagonal site is reached by moving on the defect by at about $0.19a$, from the tetrahedral site. The lower neutral charge state is achieved when the defect reaches the split ⟨110⟩.[9,43,44] For the 2+ charge state, the tetrahedral geometry is well known to be lower in energy,[9,43,45] and the defect level in the band gap is empty, so it will be used as a starting point. For the 1+ and neutral charge states, the Si_i can assume at least three geometric configurations with similar formation energies, namely, hexagonal, split ⟨110⟩, and C_{3v}.

Following Rinke *et al.*,[9] the formation energy of 1+ state for the Si_i in a supercell with N atoms, taking $\epsilon_F = E_v + \varepsilon_F + \Delta V$, is

$$E_D^f(1+,\epsilon_F) = A\left(2+ \rightarrow 1+, R_{\text{tet}}^{2+}\right) + E_{\text{rel}}\left(1+, R_{\text{tet}}^{2+} \rightarrow R_D^{1+}\right) + E_{\text{tet}}^f(2+,\epsilon_F = 0) + \epsilon_F, \quad (2)$$

where $A(2+ \rightarrow 1+, R_{\text{tet}}^{2+}) = E(1+, R_{\text{tet}}^{2+}) - E(2+, R_{\text{tet}}^{2+})$ is the electron addition energy of configuration tet 2+, first step in Fig. 2, $E_{\text{rel}}(1+, R_{\text{tet}}^{2+} \rightarrow R_D^{1+}) = E(1+, R_D^{1+}) - E(1+, R_{\text{tet}}^{2+})$ is the subsequent relaxation energy in the positive charge state (step 2), and $E_{\text{tet}}^f(2+,\epsilon_F = 0)$ is the formation energy of charge state 2+ with $\epsilon_F = 0$.

In the same way, the neutral charge state can be written as

$$E_D^f(0,\epsilon_F) = A\left(1+ \rightarrow 0, R_D^{1+}\right) + E_{\text{rel}}\left(0, R_D^{1+} \rightarrow R_D^0\right) + E_D^f(1+,\epsilon_F = 0). \quad (3)$$

The electron addition energies (A) were obtained by taking the lowest unoccupied Kohn-Sham eigenstate (LUE). However, as Eqs. (2) and (3) involve contributions arising from different calculations, the electron addition energies (from LUE) must be aligned to the same reference, which was chosen to be the valence-band maximum (VBM) in the bulk silicon (free of defects). Due to this choice, we inserted the bulk VBM energy in the electron addition energy equation (4) and added a correction term ΔV, which is responsible by the alignment

$$A\left(q \rightarrow q-1, R_D^q\right) = E_{\text{VBM}}^{\text{bulk}} + \text{LUE}\left(q, R_D^q\right) - E_{\text{VBM}}^{\text{defect}} + \Delta V. \quad (4)$$

This alignment procedure is the same one used for the electron chemical potentials (Fermi energy) in standard formation energy equations. In this way, we defined the electron addition energies $A(q \rightarrow q-1, R_D^q)$, for a charge state q and defect geometry R_D^q, as the difference between the energy of the $\text{LUE}(q, R_D^q)$ and the defect VBM energy $E_{\text{VBM}}^{\text{defect}}$, plus the VBM energy of a defect free calculation $E_{\text{VBM}}^{\text{bulk}}$, plus the correspondent ΔV, as in Eq. (4). This scheme to carry out electron addition energies will henceforth be referred as LUE-VBM procedure.

The DFT calculations were performed using the LDA and the projector-augmented wave (PAW)[46,47] method, as implemented in the Vienna *ab initio* simulation package (VASP).[48–50] We used energy cutoff of 310 eV and a $8 \times 8 \times 8$ grid of k points, in the Monkhorst-Pack scheme,[51] for 65-atom supercells and $4 \times 4 \times 4$ for 217-atom supercells, dislocated from the gamma point. The electron addition energies were taken from a band structure calculation, including gamma point. The experimental lattice parameter of 5.429 Å was used in all supercells, meaning that we do not perform volume relaxations for the different defect state configurations. The occupations of the levels were maintained free during all calculations. For the LDA-1/2 calculations, we considered the CUT parameter for silicon as obtained in Ref. 20.

III. RESULTS

We firstly focus our attention on the accuracy of Rinke's method in comparison with the total energy one for obtaining the electron addition energies considering the LDA calculations. The results are shown in Table I, for supercells with 65 and 217 atoms. In general, the LDA results of electron addition energies calculated via LUE-VBM procedure and compared to the ones calculated via total energies, presented good agreement, mainly for the 217-atom supercell. This shows that the LUE-VBM can be used straightly in the case of LDA-1/2 calculations. Now, considering the LDA-1/2 calculations, we can observe a reasonable increasing of all electron addition energies, showing a great influence of the self-energy corrections.

From these results, it is possible to calculate the corrected formation energies for the Si_i by using Eqs. (2) and (3). After that, it is necessary to add supercell size corrections to the formation energies of charged defects, in order to remove the contributions arising from the homogeneous compensation background. For this purpose, some standard DFT-LDA calculations were performed for supercells with 65, 217, and 513 atoms. The Si_i defect was placed at an undistorted Si lattice and fixed during the calculation. The formation energies

TABLE I. Results of the electron addition energies, in eV, of Si_i for different charge states and geometry, related to the bulk VBM, calculated via total energy (LDA), LUE-VBM (LDA), and LUE-VBM (LDA-1/2).

Method	LDA(E_{tot})		LDA(LUE-VBM)		LDA-1/2(LUE-VBM)	
Atoms per cell	65	217	65	217	65	217
$A(2+ \rightarrow 1+, R^{2+}_{tet})$	0.69	0.55	0.75	0.62	1.32	1.16
$A(1+ \rightarrow 0, R^{1+}_{C_{3v}})$	0.83	0.63	0.94	0.70	1.39	1.26
$A(1+ \rightarrow 0, R^{1+}_{hex})$	0.26	0.04	0.26	0.08	0.45	0.31
$A(1+ \rightarrow 0, R^{1+}_{split})$	0.10	−0.01	0.13	−0.00	0.27	0.09
$A(0 \rightarrow 1-, R^{0}_{C_{3v}})$	0.72	0.60	0.65	0.60	1.26	1.19
$A(0 \rightarrow 1-, R^{0}_{hex})$	0.79	0.60	0.67	0.62	1.15	1.23
$A(0 \rightarrow 1-, R^{0}_{split})$	0.63	0.52	0.46	0.42	0.85	0.89

were extrapolated to an infinite sized supercell by fitting a polynomial function in odd powers of $1/L$ until $1/L^3$, where L is the cubic root of the supercell volume.[52] For the 65-atom supercell, the extrapolated formation energy for the tet 2+ configuration was 3.18 eV, in good agreement with the 3.31 eV obtained by Wright and Modine[53] and 3.19 eV obtained by Rinke *et al.*[9] The 65-atom supercells corrections were 0.25, 0.23, 0.19, 0.20 eV, and the 217-atom supercell corrections were 0.13, 0.12, 0.06, and 0.13 eV, for the tet 2+, C_{3v} 1+, hex 1+ and split 1+ configurations, respectively. Note that Eqs. (2) and (3) depend on the formation energies of previous charge states, but the correction must be summed only once. For example, no correction was added to the neutral charge state although 1+ and 2+ formation energies were used in the calculations.

In Table II, are shown the formation energies calculated by LDA, via Eq. (1) and LUE-VBM procedure, combined LDA + LDA-1/2 and combined LDA + G_0W_0. The LDA results calculated via Eq. (1) are in good agreement with the ones obtained by Rinke *et al.*[9] In our calculations the C_{3v} geometry was stable only for the neutral and 1− charge states. For the 2+ and 1+ charge states, the C_{3v} goes to the tetrahedral geometry after optimisation.

Following the behavior of the electron addition energies, there is an increasing of the formation energies in all cases in different amounts. In fact, the increment arose from the correction on the electron addition energies. The increments, for the 65-atom supercells, were 0.63 eV for the 1+ charge state configurations, 1.18 eV for the neutral C_{3v}, 0.82 eV for the neutral hex and 0.79 eV for neutral split configurations. Comparing our formation energies with other theoretical ones from the literature, including G_0W_0, HSE (band-gap correction methods) and diffusion Monte Carlo (DMC), we observe that they are in the same range, and within 10% in most cases.

TABLE II. Formation energies, in eV, of the silicon self-interstitial defect for different charge states and geometry, calculated via LDA (standard method) and via combined LDA-LDA-1/2 (LUE-VBM procedure, see text), in comparison with combined LDA-G_0W_0 and LDA (usual method) results.

	This work				Other works	
Method	LDA [Eq. (1)]		LDA-1/2(LUE-VBM)		LDA	Other methods
Atoms per cell	65	217	65	217		
$E^f(2+, R^{2+}_{tet})$	2.74	3.05	...	...	2.65[a]	...
$E^f(1+, R^{1+}_{C_{3v}})$	3.70	3.86	4.33	4.48	3.00[a]	3.89[a]
$E^f(1+, R^{1+}_{hex})$	3.48	3.73	4.10	4.34	3.41[a]	4.31[a]
$E^f(1+, R^{1+}_{split})$	3.50	3.68	4.12	4.30	3.49[a]	4.41[a]
$E^f(0, R^{0}_{C_{3v}})$	3.34	3.62	4.53	4.87	3.42[b],3.36[a]	4.51[a]
$E^f(0, R^{0}_{hex})$	3.29	3.63	4.12	4.53	3.31[c],3.40[a],3.45[b],3.62[d]	4.40[a],4.82[e],4.82[f],5.13[d]
$E^f(0, R^{0}_{split})$	3.26	3.59	4.06	4.31	3.29[a],3.31[c],3.40[b],3.43[d]	4.46[a],4.64[f],4.94[d],4.96[e]
$E^f(1-, R^{1-}_{C_{3v}})$	3.47	3.71	5.27	5.56	...	...
$E^f(1-, R^{1-}_{hex})$	3.43	3.67	4.74	5.19	...	...
$E^f(1-, R^{1-}_{split})$	3.42	3.69	4.60	4.78	...	...

[a]Rinke *et al.* (G_0W_0).[9]
[b]Al-Mushadani *et al.*[44]
[c]Needs *et al.*[54]
[d]Batista *et al.* (diffusion Monte Carlo).[55]
[e]Leung *et al.* (diffusion Monte Carlo).[42]
[f]Batista *et al.* (HSE).[55]

TABLE III. Thermodynamic transitions levels, in eV, for different geometric configurations of silicon self-interstitial defect, in comparison with G_0W_0[9] calculations and experimental[56] results. The thermodynamic transition level between different charge states [$\varepsilon(q/q')$] is the Fermi energy to which the formation energies of two different charge states are equal. Where q/q' can be $+/2+$, $0/+$, and $-/0$.

Geometry	C_{3v}			hex			split			
Atoms per cell	65	217	65(G_0W_0)	65	217	65(G_0W_0)	65	217	65(G_0W_0)	Exp.
$+/2+$	0.96	1.02	1.24	0.25	0.55	0.58	0.20	0.48	0.50	0.4
$0/+$	0.93	0.95	0.62	0.08	0.15	0.09	−0.11	−0.08	0.05	0.1–0.2
$-/0$	1.44	1.29	. . .	1.29	1.26	. . .	1.00	0.99	. . .	. . .

Note that in all configurations the formation energies increase from 65 to 217 atoms per supercell. This increment occurs because of a decrease in the interaction between the defects when the size of supercell increase, which also increases the total energy per atom. In fact, a converged value of formation energies with respect to the size of supercell needs thousand of atoms,[57] but the energy difference for supercells with more than 216 atoms is no larger than 0.1 eV.[53,58] In this way we expect that the converged formation energy reaches a higher value. We found in the literature a set of experimental results, 3.12,[59] 3.6,[60] 4.68,[61] 4.75,[62] 4.95,[63] and 4.1–5.1 eV.[64] We can note that the majority is in the range of 4.1–5.1 eV, only the first two are lower, but unfortunately no explanation was given by the authors for such discrepancy.

If one adds the theoretical reaction barriers to our formation energies for 217-atom supercells, for the paths tet-hex-tet (0.12 eV) and tet-split-tet (0.18 eV), obtained from Ref. 43, we would have 4.65 eV for the hexagonal and 4.49 eV for the split. Together with the C_{3v}, 4.87 eV, these values are in excellent agreement with the experimental results cited above.

To analyze the thermodynamic transitions between different configurations of silicon defects when the Fermi energy is varied throughout the band gap, the formation energy diagrams were constructed. The results are depicted in Fig. 4. The thermodynamic transitions levels between different charge states $\varepsilon(q/q')$ correspond to the points where two lines, in Fig. 4, cross. Bracht *et al.*[56] obtained thermodynamic transition levels of Si_i in high-temperature experiments. They found levels at ∼0.1–0.2 eV and at ∼0.4 eV above valence-band maximum, labeled by them as $\varepsilon(0/+)$ and $\varepsilon(+/2+)$, respectively. From other experimental work, by Lukjanitsa *et al.*,[65] three levels were found, at 0.26, 0.46, and 0.74 eV above valence-band maximum but the authors did not say to which transitions they belong. Our results (see Table III) for 217-atom supercell in the hexagonal geometry, 0.55 eV for the $+/2+$ transition and 0.15 eV for the $0/+$ are in good agreement with the experimental ones of 0.4 and 0.1–0.2 eV by Bracht *et al.*, respectively, and with the 0.26 eV and 0.46 eV obtained by Lukjanitsa *et al.* For the split configuration, only the $+/2+$ transition result, 0.48 eV, agreed with experimental and G_0W_0 (0.50 eV)[9]. Lastly, the C_{3v} configuration has a different value according to Bracht *et al.* results and G_0W_0[9] ones, but can be compared with the 0.74 eV level obtained by Lukjanitsa *et al.*

IV. CONCLUSIONS

To summarize and conclude, we performed *ab initio* calculations for the defective supercells of 65 and 217 atoms, in four different Si_i defect configurations. We dealt separately with the two main problems for supercell defect calculations, namely, the periodic image interaction problem (size effects) (first), and the DFT (LDA and GGA) band-gap problem (second). The methodology used for the calculation of the defects formation energies involved charged systems, so that reference potential energies of the crystals had to be aligned. The above procedure did not represent a source of error as we go from the pure LDA to LDA-1/2 corrections. Although the LDA-1/2

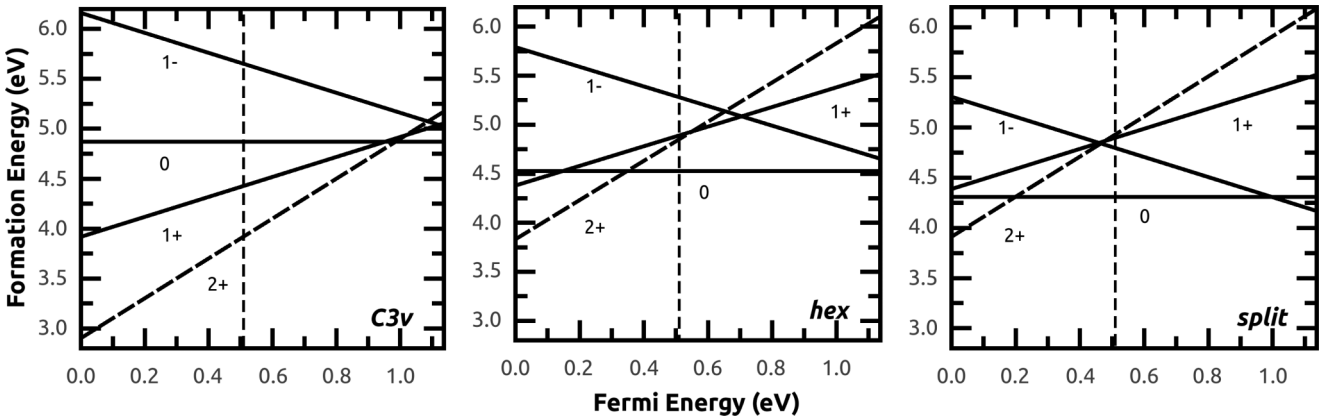

FIG. 4. Formation energies as a function of Fermi level for Si_i defect, 217-atom supercell, LDA-1/2 (solid lines) and LDA (dashed lines) results. The Fermi level is varied throughout the LDA-1/2 band gap, and vertical dashed lines indicate the LDA band-gap limits. The slopes of the segments indicate the charge states.

method was not made to calculate total energies, it improved considerably the calculations of formation energies from LDA using the electron addition energies, calculated using excited states. Regarding the two main problems listed above, we conclude that the LDA-1/2 method has shown advantages in both: it has already proven successful to overcome the band-gap problem for a number of semiconductors, and enables the use of large supercells, a fundamental condition within semiconductor defects subject. In this work, we dealt with large supercells—such an effort not achieved in literature by other methods to improve band gaps—but we state there is a real possibility of increasing even more the supercell sizes, thus tackling the second problem of defective supercells calculation.

ACKNOWLEDGMENTS

We thank L. V. C. Assali for helpful discussions. This work was developed with the help of the National Center for High-Performance Processing in São Paulo (CENAPAD), Project UNICAMP/FINEP – MCT, and supported by the Brazilian funding agencies National Council for Scientific and Technological Development (CNPq), Grant No. 141111/2011-9, and São Paulo Research Foundation (FAPESP), Grants No. 2012/50738-3 and No. 2012/14617-7.

*filipematus@gmail.com, gmsn@ita.br

[1] C. G. Van de Walle and A. Janotti, *Advanced Calculations for Defects in Materials*, edited by A. Alkauskas, P. Deák, J. Neugebauer, A. Pasquarello, and C. G. Van de Walle (Wiley-VCH, Weinheim, 2011), pp. 1–3.
[2] J. P. Perdew and A. Zunger, Phys. Rev. B **23**, 5048 (1981).
[3] J. P. Perdew, K. Burke, and M. Ernzerhof, Phys. Rev. Lett. **77**, 3865 (1996).
[4] P. Mori-Sánchez, A. J. Cohen, and W. Yang, Phys. Rev. Lett. **100**, 146401 (2008).
[5] J. P. Perdew and M. Levy, Phys. Rev. Lett. **51**, 1884 (1983).
[6] P. Deák, A. Gali, B. Aradi, and T. Frauenheim, Phys. Status Solidi B **248**, 790 (2011).
[7] R. Ramprasad, H. Zhu, P. Rinke, and M. Scheffler, Phys. Rev. Lett. **108**, 066404 (2012).
[8] A. Alkauskas and A. Pasquarello, Phys. Rev. B **84**, 125206 (2011).
[9] P. Rinke, A. Janotti, M. Scheffler, and C. G. Van de Walle, Phys. Rev. Lett. **102**, 026402 (2009).
[10] L. Hedin, Phys. Rev. **139**, A796 (1965).
[11] C. Mietze, M. Landmann, E. Rauls, H. Machhadani, S. Sakr, M. Tchernycheva, F. H. Julien, W. G. Schmidt, K. Lischka, and D. J. As, Phys. Rev. B **83**, 195301 (2011).
[12] M. J. Puska, S. Pöykkö, M. Pesola, and R. M. Nieminen, Phys. Rev. B **58**, 1318 (1998).
[13] F. Oba, A. Togo, I. Tanaka, J. Paier, and G. Kresse, Phys. Rev. B **77**, 245202 (2008).
[14] J. Weber, A. Janotti, and C. Van de Walle, Microelectron. Eng. **86**, 1756 (2009).
[15] J. L. Lyons, A. Janotti, and C. G. Van de Walle, Appl. Phys. Lett. **95**, 252105 (2009).
[16] J. R. Weber, A. Janotti, and C. G. Van de Walle, Phys. Rev. B **87**, 035203 (2013).
[17] J. Heyd, G. E. Scuseria, and M. Ernzerhof, J. Chem. Phys. **118**, 8207 (2003).
[18] J. Heyd, G. E. Scuseria, and M. Ernzerhof, J. Chem. Phys. **124**, 219906 (2006).
[19] C. G. Van de Walle and A. Janotti, Phys. Status Solidi B **248**, 19 (2011).
[20] L. G. Ferreira, M. Marques, and L. K. Teles, Phys. Rev. B **78**, 125116 (2008).
[21] L. G. Ferreira, M. Marques, and L. K. Teles, AIP Advances **1**, 32119 (2011).
[22] M. Ribeiro, Jr., L. R. C. Fonseca, and L. G. Ferreira, Phys. Rev. B **79**, 241312 (2009).
[23] A. Belabbes, A. Zaoui, and M. Ferhat, Appl. Phys. Lett. **97**, 242509 (2010).
[24] R. R. Pelá, C. Caetano, M. Marques, L. G. Ferreira, J. Furthmüller, and L. K. Teles, Appl. Phys. Lett. **98**, 151907 (2011).
[25] S. Zhang, J. Shi, M. Zhang, M. Yang, and J. Li, J. Phys. D: Appl. Phys. **44**, 495304 (2011).
[26] A. Belabbes, J. Furthmüller, and F. Bechstedt, Phys. Rev. B **84**, 205304 (2011).
[27] A. Belabbes, L. C. de Carvalho, A. Schleife, and F. Bechstedt, Phys. Rev. B **84**, 125108 (2011).
[28] R. R. Pelá, M. Marques, L. G. Ferreira, J. Furthmüller, and L. K. Teles, Appl. Phys. Lett. **100**, 202408 (2012).
[29] J. Furthmüller, F. Hachenberg, A. Schleife, D. Rogers, F. H. Teherani, and F. Bechstedt, Appl. Phys. Lett. **100**, 022107 (2012).
[30] S. Küfner, A. Schleife, B. Höffling, and F. Bechstedt, Phys. Rev. B **86**, 075320 (2012).
[31] A. Belabbes, C. Panse, J. Furthmüller, and F. Bechstedt, Phys. Rev. B **86**, 075208 (2012).
[32] J. P. T. Santos, M. Marques, L. G. Ferreira, R. R. Pelá, and L. K. Teles, Appl. Phys. Lett. **101**, 112403 (2012).
[33] M. Ribeiro, Jr., L. Ferreira, L. Fonseca, and R. Ramprasad, Mater. Sci. Eng. B **177**, 1460 (2012).
[34] M. Ribeiro, Jr., L. R. C. Fonseca, T. Sadowski, and R. Ramprasad, J. Appl. Phys. **111**, 073708 (2012).
[35] W. S. Patrocinio, M. Ribeiro, and L. R. Fonseca, Mater. Sci. Eng. B **177**, 1497 (2012).
[36] M. Ribeiro, Jr., L. R. C. Fonseca, and L. G. Ferreira, Europhys. Lett. **94**, 27001 (2011).
[37] Chris G. Van de Walle and J. Neugebauer, J. Appl. Phys. **95**, 3851 (2004).
[38] L. Kleinman, Phys. Rev. B **24**, 7412 (1981).
[39] S. Lany and A. Zunger, Modell. Simul. Mater. Sci. Eng. **17**, 084002 (2009).
[40] A. Boonchun and W. R. L. Lambrecht, Phys. Status Solidi B **248**, 1043 (2011).
[41] S. Lany and A. Zunger, Phys. Rev. B **81**, 113201 (2010).
[42] W.-K. Leung, R. J. Needs, G. Rajagopal, S. Itoh, and S. Ihara, Phys. Rev. Lett. **83**, 2351 (1999).
[43] W.-C. Lee, S.-G. Lee, and K. J. Chang, J. Phys.: Condens. Matter **10**, 995 (1998).
[44] O. K. Al-Mushadani and R. J. Needs, Phys. Rev. B **68**, 235205 (2003).
[45] R. Car, P. J. Kelly, A. Oshiyama, and S. T. Pantelides, Phys. Rev. Lett. **52**, 1814 (1984).

[46]P. E. Blöchl, Phys. Rev. B **50**, 17953 (1994).
[47]G. Kresse and D. Joubert, Phys. Rev. B **59**, 1758 (1999).
[48]G. Kresse and J. Hafner, Phys. Rev. B **47**, 558 (1993).
[49]G. Kresse and J. Hafner, Phys. Rev. B **49**, 14251 (1994).
[50]G. Kresse and J. Furthmuller, Phys. Rev. B **54**, 11169 (1996).
[51]J. Pack and H. Monkhorst, Phys. Rev. B **13**, 5188 (1976).
[52]G. Makov and M. C. Payne, Phys. Rev. B **51**, 4014 (1995).
[53]A. F. Wright and N. A. Modine, Phys. Rev. B **74**, 235209 (2006).
[54]R. J. Needs, J. Phys.: Condens. Matter **11**, 10437 (1999).
[55]E. R. Batista, J. Heyd, R. G. Hennig, B. P. Uberuaga, R. L. Martin, G. E. Scuseria, C. J. Umrigar, and J. W. Wilkins, Phys. Rev. B **74**, 121102 (2006).
[56]H. Bracht, H. H. Silvestri, I. D. Sharp, and E. E. Haller, Phys. Rev. B **75**, 035211 (2007).
[57]S. Lany and A. Zunger, Phys. Rev. B **78**, 235104 (2008).
[58]A. Shabaev, K. Hoang, D. A. Papaconstantopoulos, M. Mehl, and N. Kioussis, Comput. Mater. Sci. **79**, 888 (2013).
[59]R. Vaidyanathan, M. Y. L. Jung, and E. G. Seebauer, Phys. Rev. B **75**, 195209 (2007).
[60]Y. Shimizu, M. Uematsu, and K. M. Itoh, Phys. Rev. Lett. **98**, 095901 (2007).
[61]A. Ural, P. B. Griffin, and J. D. Plummer, Phys. Rev. Lett. **83**, 3454 (1999).
[62]H. Bracht, E. E. Haller, and R. Clark-Phelps, Phys. Rev. Lett. **81**, 393 (1998).
[63]H. Bracht, N. A. Stolwijk, and H. Mehrer, Phys. Rev. B **52**, 16542 (1995).
[64]W. Frank, U. Gösele, H. Mehrer, and A. Seeger, *Diffusion in Crystalline Solids*, edited by G. E. Murch and A. S. Nowick (Academic Press, Orlando, 1984), p. 76.
[65]V. V. Lukjanitsa, Semiconductors **37**, 404 (2003).